^{1}H NMR Study on the Self-Association of Quinacridone Derivatives in Solution

Hui Sun, Yunfeng Zhao, Zhaowei Huang, Yue Wang,* and Fei Li*

State Key Laboratory of Supramolecular Structure and Materials, Jilin University, Changchun 130012, People's Republic of China

Received: June 2, 2008; Revised Manuscript Received: September 12, 2008

The π-stacking structures and self-association thermodynamics of *N*,*N*′-di(*n*-alkyl) quinacridone derivatives (*n*-alkyl QAs) with various substituents on the side aromatic rings and different length of *n*-alkyl chains are investigated in organic solvents by ^{1}H NMR spectroscopy. The stacking geometries are built based on both the magnitudes and directions of peak shifts with concentration and solvent polarity. The intermolecular interaction between nitrogen atoms and oxygen atoms dominates the general geometrical preferences of the stacking in which the molecules are face-to-face arranged in a parallel and an antiparallel fashion, respectively. The stacking structures are little affected by the length of the *n*-alkyl chains but are regulated in an allowed range by the size and properties of the substituents. The association processes of all the *n*-alkyl QAs are enthalpically favorable at 298 K, while the relative stability of these *n*-alkyl QAs assemblies is governed mainly by the entropy of the association processes. The introduction of larger substituents and longer *n*-alkyl chains disfavors the association of the *n*-alkyl QAs, while the binding of the halogen atoms on the side aromatic rings is favorable to the association. The relative strength of the stacking interaction for the substituted *n*-alkyl QAs has not obvious correlation with the electron-donating or electron-withdrawing nature of the substituents, while it is well associated to the dispersion energy and repulsive exchange energy. The different entropy−enthalpy compensation of the halogen-substituted *n*-alkyl QAs from others may suggest different association mechanism for the two types of *n*-alkyl QAs.

Introduction

The $\pi-\pi$ interactions between aromatic units play a significant role in supramolecular chemistry and biological recognition processes, including base−base interactions of DNA,[1,2] intercalation of certain drugs into DNA,[3] side-chain interactions in proteins,[4−10] host−guest complexation,[11] self-assembly based on synthetic molecules,[12−14] and intermolecular stacking in luminescence materials or dyes.[15,16] The energetic factors that govern the strength and geometrical preference of $\pi-\pi$ interactions and the effects of substituents on $\pi-\pi$ interactions have been widely studied by the theoretical models, in particular the benzene dimer. Hunter and co-workers[17−20] interpreted the nature of $\pi-\pi$ interactions mainly based on the electrostatic effect. Kim and co-workers[21,22] showed that the relative energies between different substitituted benzene complexes are governed mainly by the electrostatic energy. However, Sherrill and co-workers[23−28] highlighted the important role of dispersion energies. They demonstrated that the effects of substituents on π-π interactions can not be explained based solely on the electrostatic interaction. Geerlings and co-workers[29] found similar results in their theoretical study of the interactions between monosubstituted benzenes with pyrimidine and imidazole.

A lot of experimental investigations of the relevant model compounds were performed to examine the stacking preference, the magnitude of $\pi-\pi$ interactions, and the influence of substituents in aromatic systems.[8,30,31] The stacking interactions of forced face-to-face arrangement in 1,8-diarylnaphthalenes with substituted aromatic rings were studied by Cozzi and Siegel[32,33] using ^{1}H NMR measurement. They found that the rotational barrier about the aryl-naphthyl bond, which depends on the strength of the parallel-stacked interaction in the ground state, increases monotonically on passing from an electron-donating to an electron-withdrawing substituent. Similar results were obtained by Rashkin and Waters.[34] They studied the offset stacking interaction using meta- and para-substituted *N*-benzyl-2-(2-fluorophenyl)-pyridinium bromides as a model system and found a rise in the barrier of rotation when the para substituent in the benzyl ring was changed from an electron-donating to an electron-accepting nature. These findings that electron-deficient rings prefer stacking interactions over electron-rich ones are in agreement with the electrostatic model by Hunter and Sanders. The importance of the electrostatic complementary was also suggested in the complexation between host and guest through aromatic interactions.[35,36] However, by use of a highly congested 1,8-diacridylnapthalene system to serve as a more robust experimental model of face-to-face $\pi-\pi$ interactions, the recent study of Mei and Wolf[37] indicated that electron-donating substituents increase binding in face-to-face $\pi-\pi$ interactions, which is in agreement with the theoretical prediction of Sherrill.

NMR spectroscopy is the most frequently used technique for investigation of aggregation due to π-stacking interaction of aromatic compounds because of its ease, precision, and the fact that the chemical shift data provide structural information for the aggregates.[38] There were many reports on this aspect of study, for instance, the aromatic π-stacking of phenylene ethynylene macrocycles in solution by Moore and co-workers,[39−41] the self-association behaviors of *m*-diethynylbenzene macrocycles in solution by Tobe and co-workers,[42] the face-to-face Dan/Ndi/Dan stack of naphthyl trimers by Iverson et al.,[43,44] a reversible interconversion between single helix and double helix of polyheterocyclic strands and $\pi-\pi$ stacking interactions between the internal heterocycles of the strands by Lehn et al.,[45] adduct formations of nucleotides and aromatic carboxylates with Pt(II)−aromatic ligand complexes by Yamauchi and co-work-

* To whom correspondence should be addressed.

10.1021/jp804846n CCC: $40.75
Published on Web 10/15/2008

ers,[46] and the $\pi-\pi$ stacking behavior in the dimer of the Ru(II)−isoeilatin complexes by Kol et al.[47]

The interaction energies involved in aromatic association are small, making it especially difficult to study this phenomenon in solution. Therefore molecules in which the $\pi-\pi$ interactions are amplified may be valuable for studying aromatic π-stacking.[41] Quinacridone derivatives, the crystal structures of which were characterized by intermolecular $\pi-\pi$ interaction,[48−50] showed a considerable strength of $\pi-\pi$ interaction in solution. The self-association of quinacridone derivatives induced detectable change in the ^{1}H and ^{13}C NMR chemical shifts.[51] Therefore, quinacridone derivatives can be used as model molecules for the study of $\pi-\pi$ interactions both in solution and solid. Moreover, QAs are widely used organic pigments that display excellent stability and a wide range of luminescent spectrum. High photoluminescent efficiency in dilute solution as well as good electrochemical stability in the solid state has allowed the fabrication of high-performance organic electroluminescent devices (OLEDs) based on QAs.[52,53] It was demonstrated that the PL and EL properties of quinacridone derivatives depend on the structures and the packing patterns of the molecules.[48,49] Accordingly, understanding on factors that affect the packing geometry and strength of quinacridone derivatives will also aid rational design and synthesis of new quinacridone derivatives for preparation of high-performance organic optical and electronic materials.

In this paper, we report the study on the self-association of *N*,*N*′-alkyl quinacridone derivatives (*n*-alkyl QAs) with different substituents on the side aromatic rings and different length of *n*-alkyl chains in organic solvents by ^{1}H NMR. The effects of the property and size of substituents and the length of *n*-alkyl chains on the π-stacking geometry and strength of $\pi-\pi$ interactions as well as the association thermodynamics are explored. Our results indicate that the stacking patterns, which are changeable only in an allowed range depending on the property and size of the substituents on the aromatic rings, are governed in general by the electrostatic interaction between nitrogen atoms of one molecule and oxygen atoms of its stacked partner. However, the relative strength of $\pi-\pi$ interactions for the *n*-alkyl QAs may be dominated by the dispersion and repulsive exchange interaction. The association processes of the *n*-alkyl QAs are enthalpically favorable, whereas the relative stability of assembly is governed mainly by the entropy change.

Materials and Methods

Quinacridone was purchased from Tokyo Kasei Kogyo Company. 3,5-Dimethylaniline, 4-(*t*-butyl)aniline, 1-bromobutane, and 1-bromodecane were purchased from Acros. Diethyl-2,5-dihydroxy-1,4-dicarboxylate, 4-fluoroaniline, and 4-bromoaniline were obtained from Aldrich. These chemicals were used as received without further purification.

The *n*-alkyl QA derivatives were synthesized according to the procedures reported previously.[48,49,54]

The samples for NMR measurements were prepared by dissolving the quinacridone derivatives in $CDCl_3$ to obtain the stock solutions with the concentrations of 60 mM for QA-C_{10} and QA-C_{16}, 20 mM for TM-QA-C_{16}, 6.7 mM for 2Br-QA-C_4, and 30 mM for others and then diluting these stock solutions with $CDCl_3$ to various concentrations. The samples with different volume percentages of polar solvent CD_3CN in $CDCl_3$ were prepared by adding an aliquot of the stocks to each tube and adding various volumes of polar solvents and $CDCl_3$ to give a total sample volume of 0.5 mL and a concentration of 7.5 mM for all QAs-C_{10} and 2F-QA-C_4 and 2.5 mM for 2Br-QA-C_4.

SCHEME 1: Structures and Denominations of the *n*-Alkyl QA Derivatives Studied

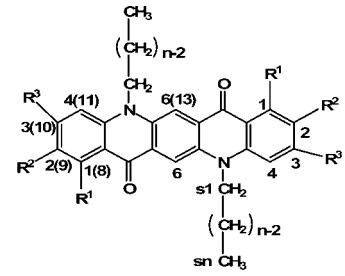

2F-QA-C_n/2Br-QA-C_n: $R^1=R^3=H$, $R^2=F/Br$, n=4

QA-C_n: $R^1=R^2=R^3=H$, n=10/16

TM-QA-C_n: $R^2=H$, $R^1=R^3=-CH_3$, n=10/16

D′Bu-QA-C_n: $R^1=R^3=H$, $R^2=-C(CH_3)_3$, n=10/16

The 1D and 2D NMR spectra were recorded on Bruker Avance 500 spectrometer using standard parameter settings. Trimethylsilane was used as the internal reference.

Results and Discussion

n-Alkyl QA derivatives used in this study are shown in Scheme 1. The atoms 8−13 on backbone rings (the numbers in parentheses of Scheme 1) are relabeled as 1−6 considering the molecular symmetry which gives rise to the same chemical shifts for H1 and H8, H2 and H9, H3 and H10, H4 and H11, and H6 and H13. The atoms on each alkyl side chain are assigned as s1, s2, s3, and so on according to the order from the N-binding CH_2 to CH_3.

Self-Association on the Basis of $\pi-\pi$ Interaction. The ^{1}H NMR spectra of these quinacridone derivatives in $CDCl_3$ at 298 K show evident upfield shifts for the signals of all aromatic protons (H1−H6) and the *n*-alkyl protons closest to the nitrogen atoms (Hs1) (see Figure S1 in Supporting Information) with increasing concentrations, suggesting that there are intermolecular associations due to $\pi-\pi$ stacking interactions in solution.[38−41,55,56] The ^{1}H NMR signals should be the weighted average between monomer and aggregate resulting from the fast intermolecular exchange on the NMR time scale at 298 K. By assumption that the monomer−dimer equilibrium is the predominant process of the self-association due to $\pi-\pi$ interactions (the assumption was proved to be rational for all the quinacridone derivatives studied according to the method previously used,[51] see the comment and Figure S2 in Supporting Information), the association constant (K) is determined by the least-square curve fitting to eq 1[38]

$$\delta_{obs} = \delta_d + (\delta_d - \delta_m)\{[1 - (8KC + 1)^{1/2}]/(4KC)\} \quad (1)$$

where δ_{obs} is the observed chemical shift, δ_m and δ_d are the chemical shifts of monomer and dimer, respectively, and C is the total concentration.

With decreasing temperature, the ^{1}H signals of the aromatic rings broaden gradually and split to two groups with different intensities at the temperature of 228 K and below for all the samples (Figure 1 and Figure S3 of Supporting Information). Both the groups of splitting signals at lower temperature shift upfield with increasing sample concentration, and the upfield part of the doublets (assigned as group II) display a more rapid upfield shift than the downfield part (assigned as group I). The intensities of the two groups of signals also change with sample concentration; the intensities of group I increase, and those of

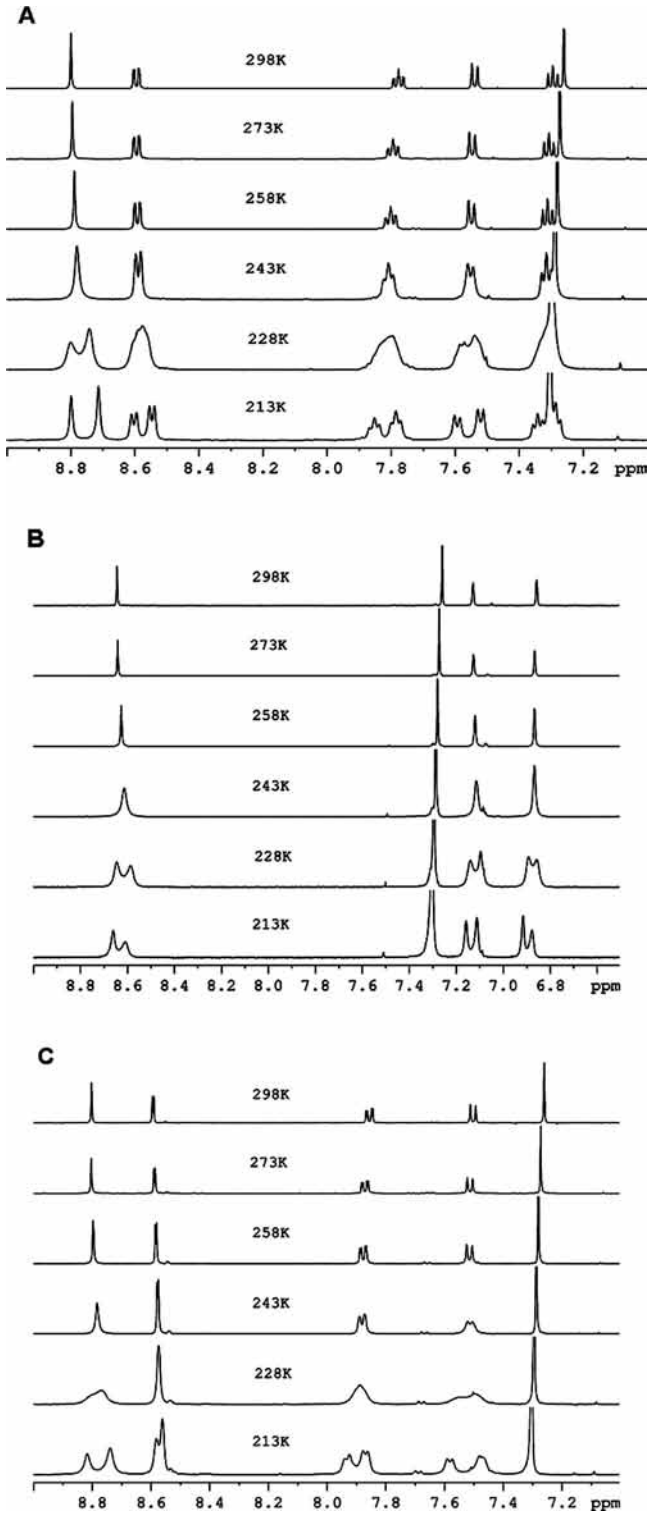

Figure 1. Aromatic region of the ^{1}H NMR spectra for QA-C_{10} (A) at 6.0 mM and TM-QA-C_{10} (B) and D^{t}Bu-QA-C_{10} (C) at 7.5 mM in $CDCl_3$ at various temperatures.

group II decrease with dilution. This reveals the existence of two self-association processes for these quinacridone derivatives in $CDCl_3$ solvent, one corresponding to the upfield part of splitting signals has a larger association constant and the other corresponding to the downfield part has a smaller association constant. The assignment of monomer and dimer for the two groups of splitting signals can be excluded because the changes in the fraction of the intensity from group I (f_I) or II ($1-f_I$) with concentration are largely different from those predicted through

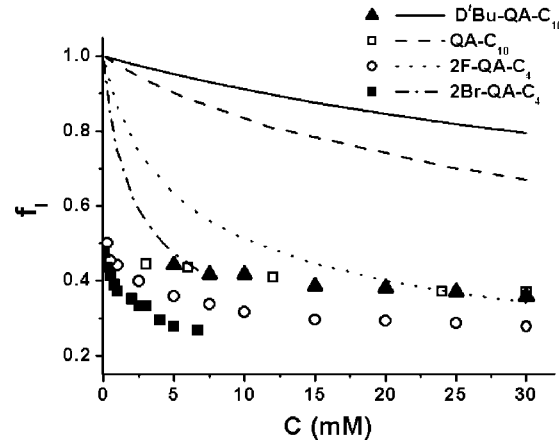

Figure 2. Concentration dependences of f_I for various *n*-alkyl QAs at 213 K. The symbols and lines represent the measured and theoretically predicted results.

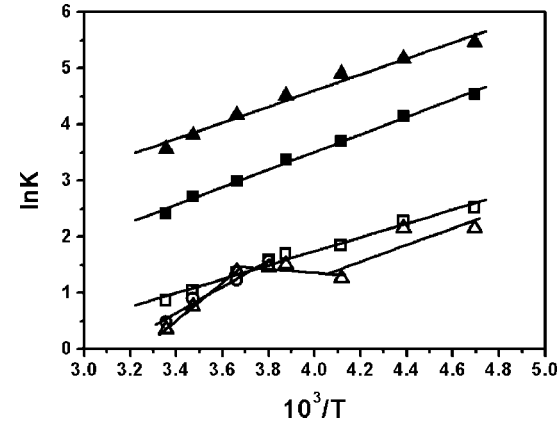

Figure 3. The van't Hoff plots for QA-C_{10} (□), TM-QA-C_{10} (○), D^{t}Bu-QA-C_{10} (Δ), 2F-QA-C_4 (■), and 2Br-QA-C_4 (▲).

the monomer−dimer equilibra (Figure 2). Therefore, two types of geometries of the $\pi-\pi$ stacking are suggested for these quinacridone derivatives. Because of the coexistence of two association processes with different association constants, as shown in Scheme 2, the apparent association constant *K* obtained

SCHEME 2: Monomer−Dimer Equilibria

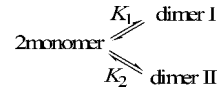

by eq 1 is the sum of the association constants of the two processes. From the *K* values at different temperatures, the thermodynamic parameters of the monomer−dimer equilibrium processes are obtained based on the van′t Hoff plots (Figure 3), as listed in Table 1.

Effect of Solvent Polarity and Geometrical Preference of $\pi-\pi$ Stacking. The addition of the polar solvent CD_3CN into $CDCl_3$ solutions of the *n*-alkyl QA samples causes the changes in the ^{1}H chemical shifts of some signals. Depending on the position of the protons in molecules, the chemical shift either increases or decreases or little changes with increasing fraction of the polar component. In general, the addition of the polar component in $CDCl_3$ results in evident upfield shift of H1/Me1 and H6 and obvious downfield shift of H4 for all the samples studied (Figure 4). The chemical shifts of other protons are less affected by the polar solvent.

TABLE 1: Thermodynamic Parameters for the Self-Associations of the Quinacridone Derivatives in $CDCl_3$ at 298 K

sample	ΔH (kJ mol^{-1})	ΔS (J mol^{-1} K^{-1})	ΔG (kJ mol^{-1})
QA-C_4[a]	-19.3 ± 2.2	-55.3 ± 7.8	-2.8 ± 0.1
TM-QA-C_4[a]	-16.3 ± 2.2	-47.3 ± 7.7	-2.2 ± 0.1
D^{t}Bu-QA-C_4[a]	-23.0 ± 4.9	-70.7 ± 17.5	-1.9 ± 0.4
2F-QA-C_4	-13.0 ± 0.4	-22.9 ± 1.6	-6.2 ± 0.1
2Br-QA-C_4	-11.9 ± 0.8	-9.2 ± 3.1	-9.1 ± 0.1
QA-C_{10}	-13.4 ± 0.1	-37.9 ± 0.3	-2.1 ± 0.0
TM-QA-C_{10}	-23.9 ± 3.6	-75.9 ± 12.9	-1.2 ± 0.3
D^{t}Bu-QA-C_{10}	-28.1 ± 0.6	-91.5 ± 2.1	-0.9 ± 0.0
QA-C_{16}	-15.3 ± 0.6	-46.5 ± 2.0	-1.4 ± 0.1

[a] The data are from ref 51.

The effect of polar solvent on the proton NMR chemical shift is in agreement with previous study on the QAs-C_4,[51] indicating that the electrostatic interaction between the carbonyl oxygen atoms of one molecule and the nitrogen atoms of the partner molecule may be predominant for the fashion of $\pi-\pi$ stacking. The solvophobic interaction of the apolar quinacridone derivatives induced by polar solvent enhances intermolecular $\pi-\pi$ interaction[41,42,57] and makes the π electrons of the carbonyl groups and the lone-pair electrons of the nitrogen atoms of the partner molecule contact more closely. As a consequence, both the abilities of the electron-withdrawing nature of the carbonyl groups and the electron-donating nature of the nitrogen atoms may be decreased, which gives rise to the upfield shift of H6 and H1 and the downfield shift of H4 relative to the chemical shifts of the corresponding protons in pure chloroform solvent. On the basis of the results of polar solvent, the two preferential stacking patterns as general geometries of the quinacridone derivatives are proposed in Figure 5. In pattern I, the molecules are face-to-face stacked in a parallel fashion and move relative to each other for about one and a half-rings along with the backbone axis. In pattern II, the molecules are also face-to-face stacked but in an antiparallel fashion with a slight slipping between layers.

Effect of Substituents. The size and property of the substituents on the side aromatic rings of the quinacridone derivatives may influence the thermodynamics of association and the geometry of $\pi-\pi$ stacking. The order of the peak shift $\Delta\delta_H$ of the aromatic protons from both group I ($\Delta\delta_{H-I}$) and II ($\Delta\delta_{H-II}$) at 213 K is used to estimate the π-stacking geometries of the *n*-alkyl QAs. The magnitude of the upfield shift $|\Delta\delta_H|$ is correlated to the position of a proton relative to the aromatic rings of the stacked partner if the ring current effect from the stacked partner is predominant for the peak shift of the proton. The larger $|\Delta\delta_H|$ is the closer the proton to the upper region of the aromatic rings of the partner molecule.

The stacking geometries of QA-C_{10}, TM-QA-C_{10}, and D^{t}Bu-QA-C_{10} are compared to examine the effect of the substituent size on π-π interactions. As shown in Figure 6A, the $|\Delta\delta_{H-I}|$ of QA-C_{10} decreases according to the order of H6, H2, H1, H3, and H4, while its $|\Delta\delta_{H-II}|$ is approximately equal for H1−H4 and larger for H6. Such orders of $|\Delta\delta_{H-I}|$ and $|\Delta\delta_{H-II}|$ outline two stacking structures of QA-C_{10} that are comparable to the general patterns proposed in Figure 5. The orders of $|\Delta\delta_{H-I}|$ and $|\Delta\delta_{H-II}|$ for TM-QA-C_{10} are similar to those of QA-C_{10} (data not shown), suggesting that the stacking geometries of TM-QA-C_{10} are similar to those of QA-C_{10}. However, D^{t}Bu-QA-C_{10} displays different orders of $|\Delta\delta_{H-I}|$ and $|\Delta\delta_{H-II}|$ from QA-C_{10} and TM-QA-C_{10}. The largest $|\Delta\delta_{H-I}|$ and $|\Delta\delta_{H-II}|$ from H4 and the smallest $|\Delta\delta_{H-I}|$ and $|\Delta\delta_{H-II}|$ from H1 (Figure 6B) as well as increasing $|\Delta\delta_{H-I}|$ and $|\Delta\delta_{H-II}|$ from Hs1 suggest two regulated stacking geometries for D^{t}Bu-QA-C_{10} in which H4 and Hs1 protons are much closer to the upper region of the aromatic rings of the partner molecule, whereas H1 is relatively far from the upper region of the partner aromatic rings. The possible patterns for the stacking of D^{t}Bu-QA-C_{10} are proposed in Figure 7. Comparing with the stacking structures of QA-C_{10} and TM-QA-C_{10}, the stacking molecules of D^{t}Bu-QA-C_{10} move (in pattern I) or turn (in pattern II) relative to each other to avoid the spatial crowding of the bulky *t*-butyl groups.

The presence of the larger size of substituents on the side aromatic rings also affects the thermodynamic processes of the association for the quinacridone derivatives. As shown in Figure 3, the association of QA-C_{10} is driven by enthalpy at the total temperature region studied. However, for D^{t}Bu-QA-C_{10} with the bulky *t*-butyl groups at position 2 on the side aromatic rings, whereas the association processes are enthalpically favorable at higher and lower temperature regions ($\Delta H = -12.4 \pm 7.9$ kJ mol^{-1}, $\Delta S = -39.1 \pm 34.9$ J mol^{-1} K^{-1}, $\Delta G = -4.1 \pm 0.5$ kJ mol^{-1} at 243−213 K, and $\Delta H = -28.1 \pm 0.6$ kJ mol^{-1}, $\Delta S = -91.5 \pm 2.1$ J mol^{-1} K^{-1}, $\Delta G = -0.9 \pm 0.0$ kJ mol^{-1} at 298−273 K), the disassociation process driven by entropy occurs in the intermediate temperature region ($\Delta H = 2.7 \pm 2.6$ kJ mol^{-1}, $\Delta S = 22.2 \pm 10.1$ J mol^{-1} K^{-1}, $\Delta G = -3.0 \pm 0.0$ kJ mol^{-1} at 273−243 K). The change in the thermodynamic behavior for D^{t}Bu-QA-C_{10} in different temperature regions is attributed to the effect of the spatial hindrance of the bulky *t*-butyl groups on the $\pi-\pi$ stacking geometry which leads to a conformational transition from higher temperature to lower temperature via a disassociation process. For TM-QA-C_{10}, only the *K* values in a temperature range of 298−258 K are obtained due to the precipitation of the sample at the lower temperature and the association in this temperature region is also enthalpically favorable.

By comparison of the thermodynamic parameters for QA-C_{10}, TM-QA-C_{10}, and D^{t}Bu-QA-C_{10} at 298 K (Table 1), one can find that the enthalpy of these association processes becomes more favorable, and the entropy more unfavorable, as the size of the substituents increases, indicating strong enthalpy−entropy compensation. The same enthalpy−entropy compensation effect was also observed for QA-C_4, TM-QA-C_4, and D^{t}Bu-QA-C_4 (Figure 8). The data in Table 1 also show that the Gibbs free energy ΔG is less favorable according to the order of QA-C_{10}, TM-QA-C_{10}, and D^{t}Bu-QA-C_{10}, i.e., the stability of the *n*-alkyl QAs assemblies is decreased according to this order. The relative association energy (or the relative stability of assembly) is governed by the entropy rather than enthalpy for these *n*-alkyl QAs, because the change tendency of ΔG on substituent size is similar to that of ΔS but opposite to that of ΔH. The extra unfavorable ΔS of TM-QA-C_{10} and D^{t}Bu-QA-C_{10} relative to unsubstituted *n*-alkyl QAs is attributed to the extra loss of the mobility of the rotatable CH_3 from the substituents on the aromatic rings in the association process.

The enthalpy change ΔH has been related to the strength of the intermolecular interaction.[58] However, it should be noted that the structures given in solution are the most stable structures in thermodynamics; the solvation could provide additional contribution to stabilize the molecular stacking besides the intrinsic molecular interaction. This should be taken into account when comparing the interaction strength based on the ΔH values. For QA-C_{10} and D^{t}Bu-QA-C_{10}, the ratios of the stacking geometry of pattern I to pattern II are nearly equal because the f_I values of the two molecules are very similar (Figure 2). The case is the same for QA-C_4 and D^{t}Bu-QA-C_4 (data not shown). If solvation difference is dominated by the ratio of the two

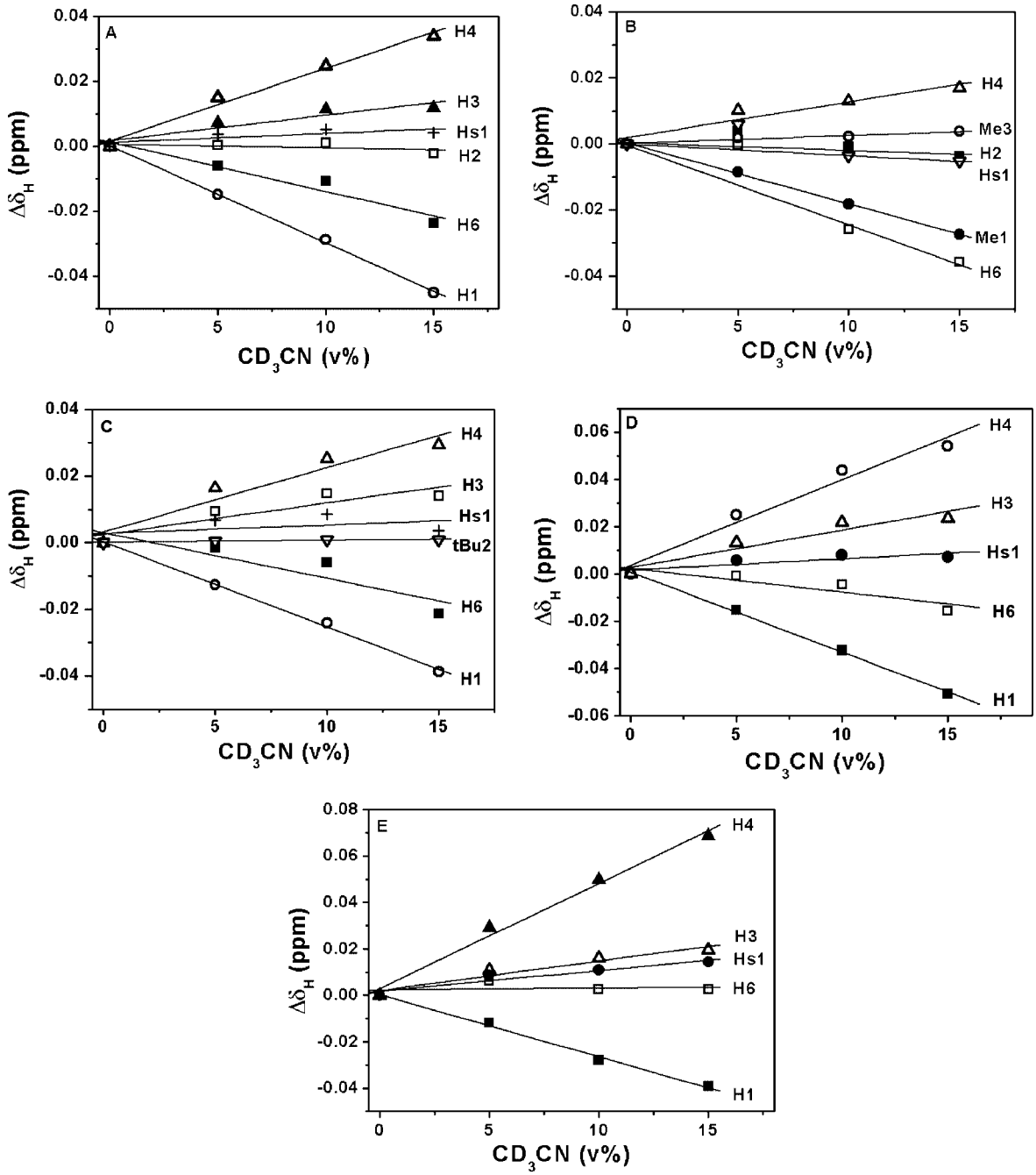

Figure 4. Peak shifts with various volume percentages of CD_3CN in $CDCl_3/CD_3CN$ mixtures for QA-C_{10} (A), TM-QA-C_{10} (B), D^{t}Bu-QA-C_{10} (C), 2F-QA-C_4 (D), and 2Br-QA-C_4 (E) at 298 K.

structure patterns and little affected by alkyl substituents, the relative interaction strength of the three *n*-alkyl QAs could be compared based on their ΔH values. It is expected that ΔH would be more unfavorable (less negative) for the assembly of D^{t}Bu-QA-C_n than QA-C_n, considering that the larger spatial hindrance of the bulky *t*-butyl group may increase the distance between the face-to-face stacking layers and decrease the strength of $\pi-\pi$ interactions. However, the ΔH is surprisingly more negative as the size of substituents on the aromatic rings increases, implying that the stacking interaction of D^{t}Bu-QA-C_n may be stronger than that of QA-C_n. In comparison with QA-C_n, the *t*-butyl groups on D^{t}Bu-QA-C_n could have more electrons to be involved in dispersion interaction, which may provide an important contribution to the stronger stacking interaction of D^{t}Bu-QA-C_n. The increase in the intermonomer distance for D^{t}Bu-QA-C_n also reduce the repulsive exchange energy from the $\pi-\pi$ overlap, which may provide an additional contribution to the stability. As the introduction of two CH_3 groups on each side aromatic rings has little effect on the stacking geometry, the increase in the dispersion force (from the substituents CH_3) and decrease in the repulsive exchange force (steric effect of CH_3) for TM-QA-C_{10} relative to QA-C_{10} could be assumed. The additional stability could be obtained if these forces are predominant.

It is noted that the ΔH values given in this study are derived from the sum of the association constants of two dimerization processes. Because K_1 and K_2 can not be obtained separately, we can not distinguish the contribution of enthalpy of one process from another. However, $K_2 > K_1$ could be assumed from the proton chemical shifts and the changes in the fractions of both processes I and II with concentration (f_I is decreased and f_{II} increased with increasing sample concentration at lower

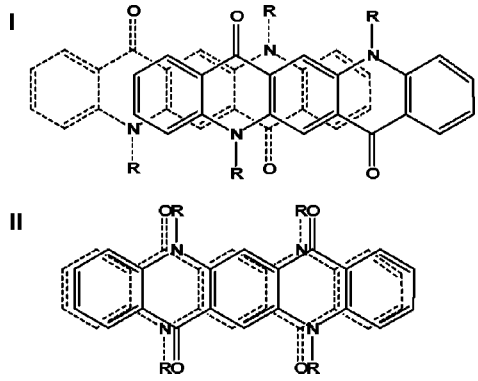

Figure 5. Proposed models of the general structures for the quinacridone derivatives.

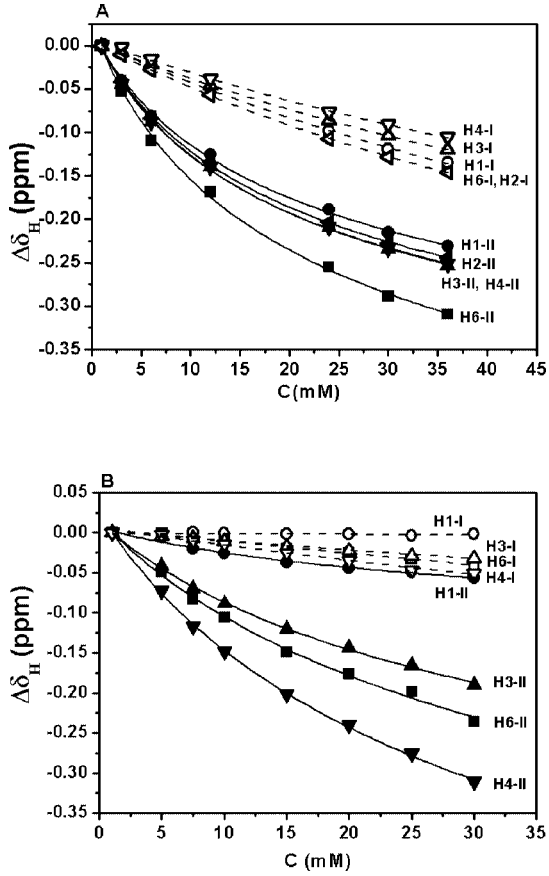

Figure 6. Concentration dependences of $\Delta\delta_{H-I}$ and $\Delta\delta_{H-II}$ for QA-C_{10} (A) and D′Bu-QA-C_{10} (B) at 213 K. $\Delta\delta_H$ is the proton chemical shift of the sample at various concentrations relative to that at the concentration of 1 mM.

temperatures). This means that the process II of the dimerization may have more contribution to the enthalpy.

The two haloids of the *n*-alkyl QAs (2X-QA-C_4) possess similar stacking patterns as predicted by the similar orders for both $|\Delta\delta_{H-I}|$ and $|\Delta\delta_{H-II}|$ of the aromatic protons at 213 K (parts A and B of Figure 9). On the basis of the orders of $|\Delta\delta_{H-I}|$ and $|\Delta\delta_{H-II}|$ of 2X-QA-C_4, H1 is expected to be slightly closer to the upper region of the partner aromatic rings in the stacking structures, while H3 and H4 are expected to be positioned relatively far from the upper region of the partner aromatic rings. The stacking in general pattern I (Figure 5) explains the orders of $|\Delta\delta_{H-I}|$ of 2X-QA-C_4 well, while the stacking structure in general pattern II can not explain the larger magnitude of upfield shift of H1 relative to H3 and H4 for 2X-QA-C_4 (parts A and

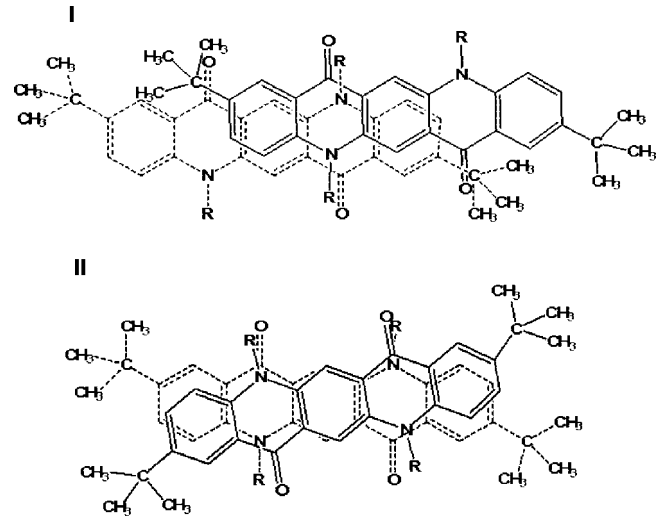

Figure 7. Proposed patterns for the stacking of D′Bu-QA-C_{10}.

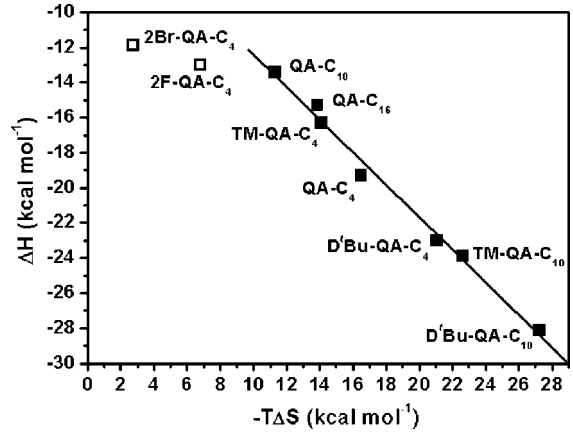

Figure 8. Enthalpy−entropy compensation plot. The solid line is the linear fit to the data sets of QA-C_n, TM-QA-C_n, and D′Bu-QA-C_n, and the slope of the fit line gives the value of -0.93 ± 0.04 for compensation.

B of Figure 9). However, a regulated structure model in which the stacked partners are slightly turned relative to each other on the backbone axis, as shown in pattern II of Figure 10, can explain the orders of $|\Delta\delta_{H-II}|$ of 2X-QA-C_4 well. The turning direction in pattern II of 2X-QA-C_4 is opposite with that of D′Bu-QA-C_n, which leads to the movement of H1 toward to the upper region of the aromatic rings of the partner compared with the pattern II of QA-C_4 (Figure 9C). The origin of the stacking regulation in the pattern II of 2X-QA-C_4 is not clear yet. Perhaps the intermolecular halogen−halogen interaction provides a contribution to stabilize this stacking structure. Although the SAPT analysis by Sherrill and co-workers showed that fluorine−fluorine interactions in substituted fluorobenzene dimers are destabilizing,[28] Boyd et al. revealed that the fluorine−fluorine interaction contributes ~14 kcal/mol of local stabilization to 1,8-difluoronaphthalene, which contains one F···F interaction, over 1,5-difluoronaphthalene, which is devoid of such an interaction, on the basis of the electron density study.[59] The halogen−halogen interactions were also found to be most common in the crystallographic structures of various polyfluorinated compounds, in which their internuclear contacts are typically shorter than the sum of the van der Waals radii for the halogen atoms, [60−63] and the nature of halogen−halogen interactions was studied as well.[64,65] It was shown that the most important contributions to the interactions of halogen atoms are

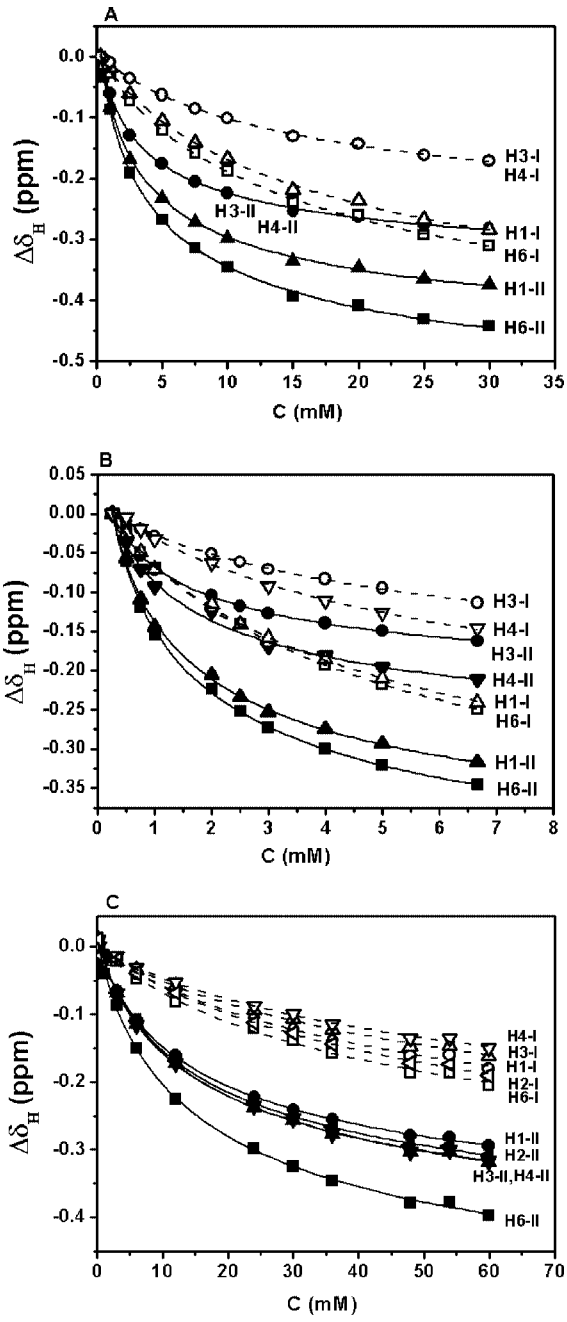

Figure 9. Concentration dependences of $\Delta\delta_{H-I}$ and $\Delta\delta_{H-II}$ for 2F-QA-C_4 (A), 2Br-QA-C_4 (B), and QA-C_4 (C) at 213 K. $\Delta\delta_H$ is the proton chemical shift of the sample at various concentrations relative to that at the concentration of 0.25 mM.

the repulsion, electrostatic, and dispersion terms, and the interactions are anisotropic because the atomic charge distribution is not spherical. The nonspherical shape of the atomic charge density was assumed to produce a decreased repulsion and thus closer halogen−halogen contacts in certain directions.[64] Therefore, the structures of van der Waals complexes and molecular crystals with halogen−halogen interactions are the compromise of many competing forces. However, the detailed mechanism on the halogen-halogen interactions has been not well understood yet.

The substitution of F and Br on C2 of the aromatic rings of QA-C_4 makes the ΔG value much more negative at 298 K (Table 1), and the ΔG value for 2Br-QA-C_4 is more negative than that for 2F-QA-C_4, suggesting that the assembly of 2Br-QA-C_4 is more stable than that of 2F-QA-C_4 and both 2X-QA-

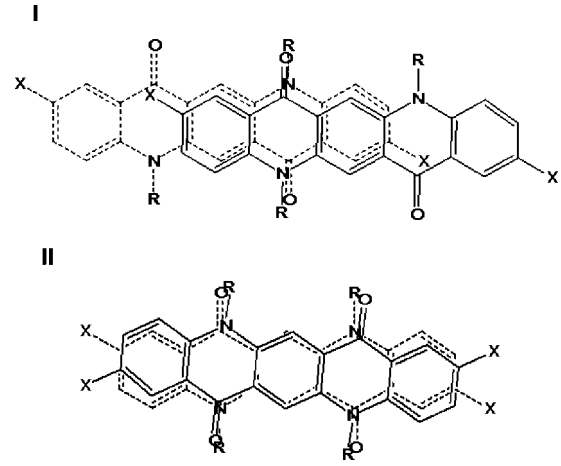

Figure 10. Proposed patterns for the stacking of 2F-QA-C_4 and 2Br-QA-C_4.

C_4 molecules are more facile to aggregate than QA-C_4. Like the *n*-alkyl QAs with different size of substituents, the relative ΔG (or the relative stability of assembly) for QA-C_4, 2F-QA-C_4, and 2Br-QA-C_4 is also governed by entropy, though the assembly processes are driven by enthalpy. However, the enthalpy−entropy compensation for the self-association of the haloids of the *n*-alkyl QAs is unexpectedly much weaker than that of other *n*-alky QAs studied (Figure 8). The enthalpic driving force is only partially compensated by the unfavorable entropic term for 2X-QA-C_4. The different enthalpy−entropy compensation for the self-association of 2X-QA-C_4 from QA-C_n, TM-QA-C_n, and D^{t}Bu-QA-C_n may suggest different association mechanism for the haloids of QA-C_4 from other *n*-alkyl QAs.

It is expected that the strength of the stacking interaction would be increased by the substitution of halogens and decreased by the substitution of both CH_3 and $C(CH_3)_3$, on the basis of the electron-donating nature of CH_3 and $C(CH_3)_3$ and the electron-withdrawing ability of F and Br in terms of Hammett's substituent constants.[66] Interestingly, the substitution of CH_3 and $C(CH_3)_3$ groups on the aromatic rings of QA-C_{10} results in more negative ΔH (larger $|\Delta H|$) of the self-association process, while the substitution of F and Br atoms on the aromatic rings gives rise to less negative ΔH (smaller $|\Delta H|$) of the self-association process (Table 1). The interaction strength of the alkyl group substituted QAs can be approximately compared by the ΔH values as their ratios of pattern II to I are very similar. However, the amount of the stacking geometry of pattern I for 2X-QA-C_4 is much less than other *n*-alkyl QA derivatives, as observed in Figure 2 where f_I of 2X-QA-C_4 is much smaller than those of both QA-C_{10} and D^{t}Bu-QA-C_{10}. The more ratio of pattern II to I of 2X-QA-C_4 may result in more solvent molecules to be disassociated form stacking molecules, which leads to less unfavorable entropy and less favorable enthalpy. The more favorable gas-phase interaction may be considerably dampened by solvent competition and entropic effects.[67] Therefore, the less negative ΔH of 2X-QA-C_4 may be resulted from the decrease in solvation but not the decrease in strength of stacking interaction. The difference in the ratio of two stacking patterns of the haloids of QA-C_4 from other *n*-alkyl QAs, and accordingly, the difference in solvation, may be the main factor that leads to the difference in their enthalpy−entropy compensation. In addition, the fact that more 2X-QA-C_4 molecules dimerize as pattern II compared with QA-C_4 molecule implies that the binding of halogen atoms makes the formation of pattern II easier. This may be attributed to the decrease in the repulsion

of π electrons due to the electron-withdrawing effect of halogen atoms. Relative to the geometry of pattern I, the pattern II of 2X-QA-C_4 could have more dispersion energy and repulsive exchange energy.

Effect of *n*-Alkyl Length. By comparison of Figure 6A and Figure 9C, it is found that both the orders of $|\Delta\delta_{H-I}|$ and $|\Delta\delta_{H-II}|$ from various aromatic protons of QA-C_4 are similar to those of QA-C_{10}. Because of the occurrence of precipitation for the sample QA-C_{16} even at lower concentration, only the ^{1}H NMR spectra at the sample concentrations of 1, 3, and 6 mM were obtained for this sample. The magnitudes of the peak shift $|\Delta\delta_{H-I}|$ and $|\Delta\delta_{H-II}|$ from various aromatic protons of QA-C_{16} at the concentration of 6 mM relative to those at 1 mM at 213 K show the coincident orders with those of QA-C_4 and QA-C_{10} (see Table S1 of Supporting Information). The results indicate that the length of the n-alkyl chains binding on the N atoms has little effect on the stacking geometry of the quinacridone derivatives.

As expected, the ΔG value becomes less favorable as the length of the *n*-alkyl chain is increased, suggesting that the longer *n*-alkyl chain disfavors the association process of the *n*-alkyl QAs. Furthermore, as the length of the *n*-alkyl chain is increased, the ΔS value is more unfavorable, and the ΔH value more favorable for all QA-C_n, TM-QA-C_n, and D^{t}Bu-QA-C_n, only with exception of QA-C_4. These results indicate that there is a strong enthalpy−entropy compensation for the association processes of the *n*-alkyl QAs (Figure 10) and that the entropy change may govern the relative stability of the association. The longer *n*-alkyl chain leads to more amount of loss of the *n*-alkyl chain mobility upon association, which results in the less favorable ΔG. On the basis of the ΔH values, the stacking interaction may increase with increasing length of *n*-alkyl chain (the split NMR spectra at low temperature show that the length of *n*-alkyl chains has little effect on the ratio of two stacking patterns). The introduction of longer *n*-alkyl chains could increase the dispersion interaction and decrease the repulsive energy component as intermonomer distance could be enlarged. This suggests that the relative energy of the stacking interaction for the *n*-alkyl QAs with different length of *n*-alkyl chains may be governed mainly by the dispersion energy and the repulsive exchange energy.

Conclusions

The quinacridone derivatives are self-associated as dimers in a $CDCl_3$ solvent based on the $\pi-\pi$ stacking interactions. The geometry of the stacking is governed by the electrostatic interaction between the nitrogen atoms of one molecule and the oxygen atoms of its stacking partner. The intermolecular nitrogen−oxygen pairing yields two stable face-to-face stacking structures with a parallel and an antiparallel fashion in general, respectively. The geometry is regulated more or less depending on the size and property of the substituents on the side aromatic rings.

All the self-association processes for the substituted *n*-alkyl QAs are enthalpically favorable at the temperatures studied except for D^{t}Bu-QA-C_n, whose self-association is driven by enthalpy in the higher and lower temperature regions but by entropy in the intermediate temperature region. The abnormality for D^{t}Bu-QA-C_n is attributed to the spatial hindrance of the bulky *t*-butyl group when the stacking structure is regulated from higher temperature to lower temperature. The increase both in the size of the substituents and in the length of the *n*-alkyl chain decreases the stability of the *n*-alkyl QAs assembly, while the substitution of halogens with electron-withdrawing nature increases the stability of the *n*-alkyl QAs assembly. The relative stability of these *n*-alkyl QAs assemblies is governed by the entropy change rather than the enthalpy change of the association processes. The relative strength of the stacking interaction, associated to the enthalpy change (ΔH), for the substituted *n*-alkyl QAs, does not have an obvious correlation with the electron-donating or electron-withdrawing nature of the substituents, while it is well associated to the dispersion energy and repulsive exchange energy. The entropy−enthalpy compensation of the haloids of the *n*-alkyl QAs is different from that of other *n*-alkyl QAs, suggesting that the thermodynamic mechanism of the association processes between the two types of *n*-alkyl QAs may be different.

Acknowledgment. This work was financially supported by the National Basic Research Program of China (2003CB615802), the National Natural Science Foundation of China (50733002), and the PCSIRT (IRT0422).

Supporting Information Available: The estimation of the aggregation number, the relative shift data for QA-C_{16} at 213 K, the plots of $\Delta\delta_H$ vs concentration, and some ^{1}H NMR spectra. This information is available free of charge via the Internet at http://pubs.acs.org.

References and Notes

(1) Rappe, A. K.; Bernstein, E. R. *J. Phys. Chem. A* **2000**, *104*, 6117.
(2) Guckian, K. M.; Schweitzer, B. A.; Ren, R. X.-F.; Sheils, C. J.; Tahmassebi, D. C.; Kool, E. T. *J. Am. Chem. Soc.* **2000**, *122*, 2213.
(3) Boehr, D. D.; Farley, A. R.; Wright, G. D.; Cox, J. R. *Chem. Biol.* **2002**, *9*, 1209.
(4) Butterfield, S. M.; Patel, P. R.; Waters, M. L. *J. Am. Chem. Soc.* **2002**, *124*, 9751.
(5) Viguera, A. R.; Serrano, L. *Biochemistry* **1995**, *34*, 8771.
(6) Padmanabhan, S.; Jiménez, M. A.; Laurents, D. V.; Rico, M. *Biochemistry* **1998**, *37*, 17318.
(7) Aravinda, S.; Shamala, N.; Das, C.; Sriranjini, A.; Karle, I. L.; Balaram, P. *J. Am. Chem. Soc.* **2003**, *125*, 5308.
(8) Waters, M. L. *Biopolymers* **2004**, *76*, 435.
(9) Tatko, C. D.; Waters, M. L. *J. Am. Chem. Soc.* **2002**, *124*, 9372.
(10) Meurissea, R.; Brasseura, R.; Thomas, A. *Biochim. Biophys. Acta* **2003**, *1649*, 85.
(11) Balzani, V.; Bandmann, H.; Ceroni, P.; Giansante, C.; Hahn, U.; Klärner, F.-G.; Müller, U.; Müller, W. M.; Verhaelen, C.; Vicinelli, V.; Vögtle, F. *J. Am. Chem. Soc.* **2006**, *128*, 637.
(12) Bagryanskaya, I. Y.; Gatilov, Y. V.; Maksimov, A. M.; Platonov, V. E.; Zibarev, A. V. *J. Fluor. Chem.* **2005**, *126*, 1281.
(13) Zhang, W.; Horoszewski, D.; Decatur, J.; Nuckolls, C. *J. Am. Chem. Soc.* **2003**, *125*, 4870.
(14) Tanatani, A.; Yamaguchi, K.; Azumaya, I.; Fukutomi, R.; Shudo, K.; Kagechika, H. *J. Am. Chem. Soc.* **1998**, *120*, 6433.
(15) Wang, W.; Han, J. J.; Wang, L.-Q.; Li, L.-S.; Shaw, W. J.; Li, A. D. Q. *Nano Lett.* **2003**, *3*, 455.
(16) Thetforda, D.; Cherrymanb, J.; Chorltonc, A. P.; Docherty, R. *Dyes Pigments* **2004**, *63*, 259.
(17) Hunter, C. A.; Sanders, J. K. M. *J. Am. Chem. Soc.* **1990**, *112*, 5525.
(18) Hunter, C. A. *Angew. Chem., Int. Ed.* **1993**, *32*, 1584.
(19) Hunter, C. A. *Chem. Soc. Rev.* **1994**, *23*, 101.
(20) Cockroft, S. L.; Hunter, C. A.; Lawson, K. R.; Perkins, J.; Urch, C. J. *J. Am. Chem. Soc.* **2005**, *127*, 8594.
(21) Lee, E. C.; Hong, B. H.; Lee, J. Y.; Kim, J. C.; Kim, D.; Kim, Y.; Tarakeshwar, P.; Kim, K. S. *J. Am. Chem. Soc.* **2005**, *127*, 4530.
(22) Lee, E. C.; Kim, D.; Tarakeshwar, P. P.; Hobza, P.; Kim, K. S. *J. Phys. Chem. A* **2007**, *111*, 3446.
(23) Sinnokrot, M. O.; Valeev, E. F.; Sherrill, C. D. *J. Am. Chem. Soc.* **2002**, *124*, 10887.
(24) Sinnokrot, M. O.; Sherrill, C. D. *J. Phys. Chem. A* **2003**, *107*, 8377.
(25) Sinnokrot, M. O.; Sherrill, C. D. *J. Phys. Chem. A* **2004**, *108*, 10200.
(26) Sinnokrot, M. O.; Sherrill, C. D. *J. Am. Chem. Soc.* **2004**, *126*, 7690.
(27) Sinnokrot, M. O.; Sherrill, C. D. *J. Phys. Chem. A* **2006**, *110*, 10656.
(28) Ringer, A. L.; Sinnokrot, M. O.; Lively, R. P.; Sherrill, C. D *Chem.−Eur. J.* **2006**, *12*, 3821.

(29) Mignon, P.; Loverix, S.; Geerlings, P. *Chem. Phys. Lett.* **2005**, *401*, 40.
(30) Meyer, E. A.; Castellano, R. K.; Diederich, F. *Angew. Chem., Int. Ed.* **2003**, *42*, 1210.
(31) Hunter, C. A.; Lawson, K. R.; Perkins, J.; Urch, C. J. *J. Chem. Soc., Perkin Trans.* **2001**, *2*, 651.
(32) Cozzi, F.; Cinquini, M.; Annunziata, R.; Dwyer, T.; Siegel, J. S. *J. Am. Chem. Soc.* **1992**, *114*, 5729.
(33) Cozzi, F.; Siegel, J. S. *Pure Appl. Chem.* **1995**, *67*, 683.
(34) Rashkin, M. J.; Waters, M. L. *J. Am. Chem. Soc.* **2002**, *124*, 1860.
(35) Ferguson, S. B.; Diederich, F. *Angew. Chem., Int. Ed.* **1986**, *25*, 1127.
(36) Shepodd, T. J.; Petti, M. A.; Dougherty, D. A. *J. Am. Chem. Soc.* **1988**, *110*, 1983.
(37) Mei, X.; Wolf, C. *J. Org. Chem.* **2005**, *70*, 2299.
(38) Martin, R. B. *Chem. Rev.* **1996**, *96*, 3043.
(39) Zhang, J.; Moore, J. S. *J. Am. Chem. Soc.* **1992**, *114*, 9701.
(40) Shetty, A. S.; Zhang, J.; Moore, J. S. *J. Am. Chem. Soc.* **1996**, *118*, 1019.
(41) Lahiri, S.; Thompson, J. L; Moore, J. S. *J. Am. Chem. Soc.* **2000**, *122*, 11315.
(42) Tobe, Y.; Utsumi, N.; Kawabata, K.; Nagano, A.; Adachi, K.; Araki, S.; Sonoda, M.; Hirose, K.; Naemura, K. *J. Am. Chem. Soc.* **2002**, *124*, 5350.
(43) Gabriel, G. J.; Iverson, B. L. *J. Am. Chem. Soc.* **2002**, *124*, 15174.
(44) Gabriel, G. J.; Sorey, S.; Iverson, B. L. *J. Am. Chem. Soc.* **2005**, *127*, 2637.
(45) Barboiu, M.; Vaughan, G.; Kyritsakas, N.; Lehn, J.-M. *Chem.−Eur. J.* **2003**, *9*, 763.
(46) Yajima, T.; Maccarrone, G.; Takani, M.; Contino, A.; Arena, G.; Takamido, R.; Hanaki, M.; Odani, Y. F. A.; Yamauchi, O. *Chem.−Eur. J.* **2003**, *9*, 3341.
(47) Bergman, S. D.; Reshef, D.; Frish, L.; Cohen, Y.; Goldberg, I.; Kol, M. *Inorg. Chem.* **2004**, *43*, 3792.
(48) Ye, K. Q.; Wang, J.; Sun, H.; Liu, Y.; Mu, Z. C.; Li, F.; Jiang, S. M.; Zhang, J. Y.; Zhang, H. X.; Wang, Y.; Che, C. M. *J. Phys. Chem. B* **2005**, *109*, 8008.
(49) Wang, J.; Zhao, Y. F.; Dou, C. D.; Sun, H.; Xu, P.; Ye, K. Q.; Zhang, J. Y.; Jiang, S. M.; Li, F.; Wang, Y. *J. Phys. Chem. B* **2007**, *111*, 5082.
(50) De Feyter, S.; Gesquière, A.; Schryver, F. C. D. *Chem. Mater.* **2002**, *14*, 989.
(51) Sun, H.; Ye, K.; Wang, C.; Qi, H.; Li, F.; Wang, Y. *J. Phys. Chem. A* **2006**, *110*, 10750.
(52) Shi, J.; Tang, C. W. *Appl. Phys. Lett.* **1997**, *70*, 1665.
(53) Gross, E. M.; erson, J. D.; Slaterbeck, A. F.; Thayumanavan, S.; Barlow, S.; Zhang, Y.; Marder, S. R.; Hall, H. K.; Nabor, M. F.; Wang, J. F.; Mask, E. A.; Armstrong, N. R.; Wightman, R. M. *J. Am. Chem. Soc.* **2000**, *122*, 4972.
(54) Keller, U.; Müllen, K.; Feyter, S. De; Schryver, F. C. *Adv. Mater.* **1996**, *8*, 490.
(55) Höger, S.; Bonrad, K.; Mourran, A.; Beginn, U.; Möller, M. *J. Am. Chem. Soc.* **2001**, *123*, 5651.
(56) Nakamura, K.; Okubo, H.; Yamaguchi, M. *Org. Lett.* **2001**, *3*, 10979.
(57) Cubberley, M. S.; Iverson, B. L. *J. Am. Chem. Soc.* **2001**, *123*, 7560.
(58) Krishnamurthy, V. M.; Bohall, B. R.; Semetey, V.; Whitesides, G. M. *J. Am. Chem. Soc.* **2006**, *128*, 5802.
(59) Matta, C. F.; Castillo, N.; Boyd, R. J. *J. Phys. Chem. A* **2005**, *109*, 3669.
(60) Olejniczak, A.; Katrusiak, A.; Vij, A *J. Fluor. Chem.* **2008**, *129*, 173.
(61) Gupta, O. D.; Twamley, B.; Kirchmeier, R. L.; Shreeve, J. M. *J. Fluor. Chem.* **2000**, *106*, 199.
(62) Choudhury, A. R.; Urs, U. K.; Row, T. N. G.; Nagarajan, K. *J. Mol. Struct.* **2002**, *605*, 71.
(63) Jckel, C.; Salwiczek, M.; Koksch, B. *Angew. Chem., Int. Ed.* **2006**, *45*, 41983.
(64) Price, S. L.; Stone, A. J.; Lucas, J.; Rowland, R. S.; Thomley, A. E. *J. Am. Chem. Soc.* **1994**, *116*, 4910.
(65) Desiraju, G. R.; Parthasarathy, R. *J. Am. Chem. Soc.* **1989**, *111*, 8725.
(66) Shieh, D. J.; Lee, S.-T.; Yim, Y.-C.; Lin, S. H.; Eyring, H. *Proc. Nat. Acad. Sci. USA* **1975**, *72*, 452.
(67) Jorgensen, W. L.; Severance, D. L. *J. Am. Chem. Soc.* **1990**, *112*, 4768.

JP804846N